IEICE TRANS. ELECTRON., VOL.E92–C, NO.11 NOVEMBER 2009

INVITED PAPER *Special Section on Electronic Displays*

Degradation Analysis of Blue Phosphorescent Organic Light Emitting Diode by Impedance Spectroscopy and Transient Electroluminescence Spectroscopy

Toshinari OGIWARA[†a)], **Jun-ichi TAKAHASHI**[†], **Hitoshi KUMA**[†], **Yuichiro KAWAMURA**[†], **Toshihiro IWAKUMA**[†], ***and*** **Chishio HOSOKAWA**[†], ***Nonmembers***

SUMMARY We carried out degradation analysis of a blue phosphorescent organic light emitting diode by both impedance spectroscopy and transient electroluminescence (EL) spectroscopy. The number of semicircles observed in the Cole-Cole plot of the modulus became three to two after the device was operated for 567 hours. Considering the effective layer thickness of the initial and degraded devices did not change by degradation and combining the analysis of the Bode-plot of the imaginary part of the modulus, the relaxation times of emission layer and hole-blocking with electron transport layers changed to nearly the same value by the increase of the resistance of emission layer. Decay time of transient EL of the initial device was coincident with that of the degraded one. These phenomena suggest that no phosphorescence quenching sites are generated in the degraded device, but the number of the emission sites decrease by degradation.

key words: *degradation analysis, blue phosphorescent OLED, impedance spectroscopy, transient electroluminescence spectroscopy*

1. Introduction

Organic light emitting diode (OLED) is a complex device with a multi-layer structure. The J-V characteristics are the over-all result of injection and transport of carriers through the layers. The OLED consists of different functional parts, such as hole injection, hole transport, electron injection, electron transport, and emission layer, which have different transport properties. It is important to characterize where the change of device dynamics, and what the type of change of the physical and chemical processes occur [1]–[4]. From the view of carrier transport dynamics, each layer can be regarded as a unit composed of a capacitance and a resistance. The dynamics of each unit can be analyzed separately by an impedance spectroscopy (IS). For example, Brütting and Riess et al. noted that position dependence of the carrier conductivity in OLED using IS [5]–[10]. Even though IS is an effective method to study transport dynamics, it is difficult to elucidate the luminescence dynamics by it. The quenching dynamics must be studied by transient electroluminescence (EL) spectroscopy [11], [12].

In this paper, we report results of experimental analysis about degradation mechanisms of a blue phosphorescent OLED by IS and transient EL spectroscopy. Combining these techniques, we discuss the physical interpretations of resistance, capacitance, and exciton dynamics in initial and degraded OLEDs.

Manuscript received February 26, 2009.
Manuscript revised June 1, 2009.

[†]The authors are with Idemitsu Kosan Co., Ltd., Sodegaurashi, 299-0293 Japan.
a) E-mail: toshinari.ogiwara@si.idemitsu.co.jp

DOI: 10.1587/transele.E92.C.1334

2. Experiments

The OLED structures in this study were ITO/HT-1(100)/PBH-1:PBD-1(30;x%)/HB-1(25)/Alq_3(5)/LiF/Al.

Here, HT-1 [13], PBH-1, PBD-1, HB-1, and Alq_3 are a hole transport, host, blue phosphorescent dopant, hole-blocking, and electron transport materials, respectively. Numbers in parentheses are the layer thickness in nm. Two types of devices, with and without the dopant (x = 0 and 7.5 wt%), were made for comparison. Furthermore, we fabricated hole-only devices as follows, in order to study the hole transport characteristics of emission layer, ITO/HT-1(5)/PBH-1:PBD-1(95;x%)/Al.

The organic materials and the metal cathode were evaporated on ITO/glass substrates in vacuum. After completion of the evaporation, the devices were encapsulated in nitrogen gas. The emitting areas were squares of 0.06 cm^2, which were determined by the aperture of mask for the cathode evaporation. IS measurements were carried out using a Solartron 1260 impedance analyzer with a 1296 dielectric interface in the frequency sweep range from 100 mHz to 1 MHz at room temperature. The AC oscillation amplitude was 100 mV.

In Cole-Cole plot of modulus (M-plot), several semicircles can be observed in the low voltage region below the critical voltage of emission, because the OLED has several layers which have totally different mobilities and similar dielectric constants. Their equivalent circuit can be well represented by serially connected Randle units, which consists of capacitance (C) and resistance (R) in parallel. The complex modulus of equivalent circuit of Fig. 1 is defined as equation 1, where N is the number of the Randle units, ω is the angular frequency, and Z is the complex impedance. The diameters of the semicircles are the inverse of the capacitance of each Randle unit. Typical plots are shown in Fig. 1 in the case of two Randle units case.

$$M \equiv \sum_{i=1}^{N=2} j\omega Z_i = \sum_{i=1}^{N=2} \frac{1}{C_i}\left(1 - \frac{1}{1 + j\omega C_i R_i}\right) \quad (1)$$

$$\approx \sum_{i=1}^{N=2} \frac{1}{C_i} (\omega \to \infty) \quad (2)$$

$$\sim M_{HighFrequency} \approx \frac{1}{C} = \frac{1}{\varepsilon} \cdot \frac{d}{S} \propto d \quad (3)$$

The diameter of the semicircle of the M-plot has a clear physical meaning, i.e. the effective layer thickness when it is scaled by the area. Comparing the effective layer thickness with the designed layer thickness, it is easy to assign which semicircles correspond to the fabricated layers. Moreover, we can see the change of conductivity of each layer by analyzing the Bode-plot of the imaginary part of the modulus. The peak frequencies of it are the inverse of the product of C and R of the layers, i.e. the relaxation times (τ=CR). Because C is mostly independent of bias voltage, the peak shift implies the change of the conductivity [14], [15]. These two graphical representations are quite useful to see the change of the layer-to-layer carrier dynamics of multi-layer OLED.

Transient EL responses were monitored by a photomultiplier tube (Hamamatsu Photonics K.K. R928). The photocurrents were entered directly into an input channel of a digital oscilloscope (Tektronix, Inc 2440) with an impedance of 50 Ω. The devices were connected serially to a pulse generator (Agilent Technologies, Inc. 8114 A) and another channel of the oscilloscope with the impedance of 50 Ω. The repetition rate was 20 Hz and the pulse width was 500 μs. The signals of photocurrent were averaged on the oscilloscope till the signals became sufficiently smooth and then they were transferred to a PC. The photocurrents were acquired under 0.1 μs/div, 2 μs/div, and 20 μs/div and the data were joined in one sequence.

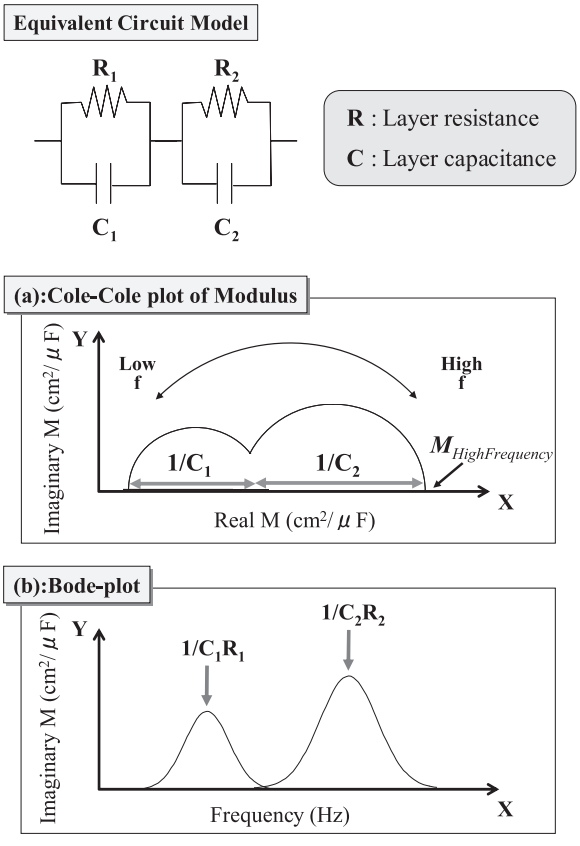

Fig. 1 Plot-models of the equivalent circuit of parallelly connected capacitance and resistance. (a) Cole-Cole plot of Modulus, (b) Bode-plot.

3. Results and Discussions

3.1 Performance of OLED

Figure 2 shows the J-V characteristics of the PBD-1 doped and non-doped devices. Shift of threshold voltage about 0.4 V was observed with non-doped one. The same phenomena were also observed with the hole-only devices (Fig. 3). This fact shows that the blue phosphorescent dopant PBD-1 assists the hole injection to emission layer.

Figure 4 shows the EL spectra of the PBD-1 doped and non-doped devices at 1 mA/cm^2, and PL spectra of PBD-1, HT-1, PBH-1 and HB-1. PBD-1 was dissolved in dichloromethane (Concentration: 1×10^{-4} mol/l). Neat 100 nm thick films of HT-1, PBH-1 and HB-1 were deposited by the conventional thermal evaporation under vacuum onto a quartz plates. All PL spectra were recorded by HITACHI F-7000 spectrometer. The onset voltage of PBD-1 doped device was 5.86 V, which was lower than that of the non-doped one, 6.55 V. This is related to improvement

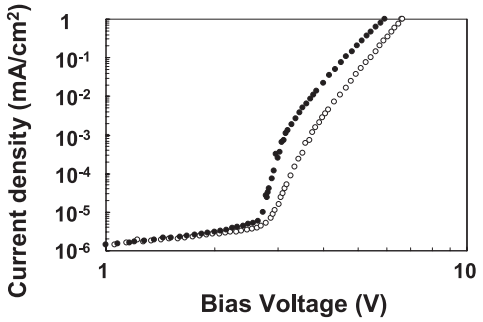

Fig. 2 J-V characteristics of the PBD-1 doped (filled) and non-doped (open) devices.

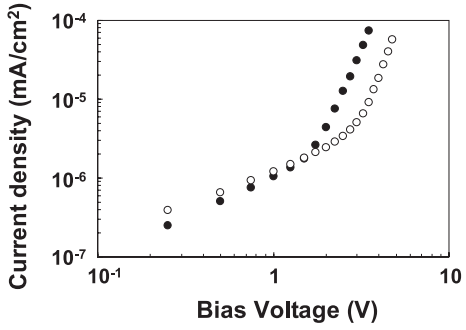

Fig. 3 J-V characteristics of the PBD-1 doped (filled) and non-doped (open) hole-only devices.

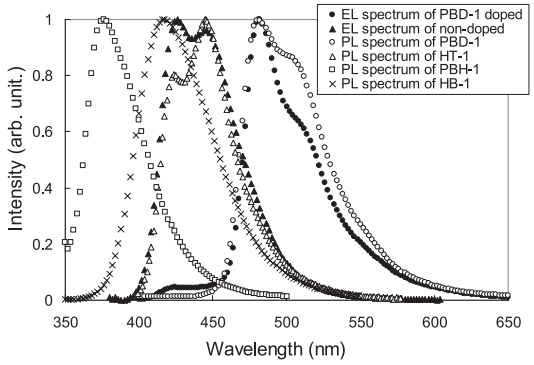

Fig. 4 Normalized EL spectra for the PBD-1 doped and PBD-1 non doped devices at 1 mA/cm^2. Normalized PL spectra of PBD-1, HT-1, PBH-1, and HB-1 (Excitation wavelength: 317 nm).

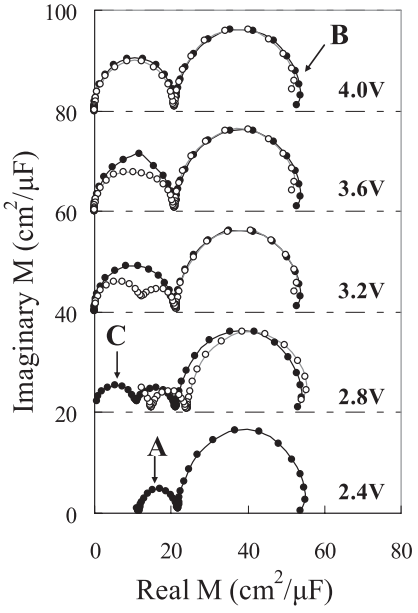

Fig. 5 Cole-Cole plots of Modulus the PBD-1 doped (filled-circle) and non-doped (open-circle) devices. Each data is shifted upwards by 20 cm^2/μF for clarity.

of hole injection by doping PBD-1. The EL spectrum of the PBD-1 doped device was similar to the PL spectrum of PBD-1. This means that electrons injected into the PBH-1 layer from HB-1 side would recombine with holes immediately, and PBD-1 would emit light. On the other hand, EL spectrum of the non-doped device was coincident with PL spectrum of HT-1. We can cite the two reasons of HT-1 emission as follows; first, most of electrons pass through emission layer to hole transport layer without recombining with holes in the emission layer. The electrons have migrated to the HT-1 side. Second, the excitons generated by recombination in PBH-1 also transfer to the HT-1 side by Förster energy mechanism because the energy gap of singlet of PBH-1 is larger than that of HT-1.

Figure 5 shows the M-plot of the PBD-1 doped and non-doped devices. Three semicircles were observed in the

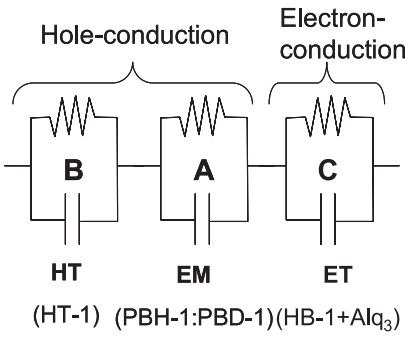

Fig. 6 Equivalent circuit model of PBD-1 doped and non-doped devices.

Table 1 The performance of the PBD-1 doped devices (10 mA/cm^2).

	Voltage (V)	Efficiency (cd/A)	CIE (x,y)	External Quantum Efficiency (%)
Initial device	7.83	14	(0.165,0.398)	6.29
Degraded device	8.37	7.5	(0.175,0.412)	3.26

M-plot. This fact shows that the equivalent circuit of the device can be expressed by three units connected serially, each unit of which are composed of C and R connected in parallel. We calculated the effective layer thickness by assuming the effective dielectric constant as $\varepsilon = 3$. Comparing them with the designed layer thickness and the conductivity of each layer, the semicircles A, B, and C are assigned to the emission layer (EM), the hole transport layer (HT), and the coalesced layer of hole-blocking layer and electron transport layer (ET). Here, the hole mobility of HT-1, PBH-1 are 6.5×10^{-4} and 1.2×10^{-4} (cm^2/Vs), and the electron mobility of HB-1, Alq_3 are 1.6×10^{-5} and 2.0×10^{-6} (cm^2/Vs), respectively. These are measured by the time of flight method at around 500 (V/cm)$^{1/2}$. Considering mobilities of HT, EM, ET materials, the semicircles A and B are signals from hole conduction, and the semicircle C is a signal from electron conduction. Three semicircles of the PBD-1 doped device were observed in lower voltage side than non-doped one. The same phenomena were also observed with J-V characteristics of the PBD-1 doped and non-doped devices.

In conclusion, it is shown that the role of PBD-1 is not only luminescence species but also assisting species of hole injection to the emission layer in the phosphorescent OLED.

3.2 Degradation Analysis by IS

The performances of the initial and degraded devices of the PBD-1 doped device are shown in Table 1. The degraded device was operated at the initial luminance of 1,000 cd/m^2 for 567 hours, which is referred to as LT50.

Figure 7 shows the M-plot of the initial and degraded devices. The semicircles X, Y and Z are assigned to EM, HT and ET, respectively. In contrast to the initial device, M-plot of the degraded device at 2.8 V shows only two semicircles. From the correspondence between the diameter of the semi-

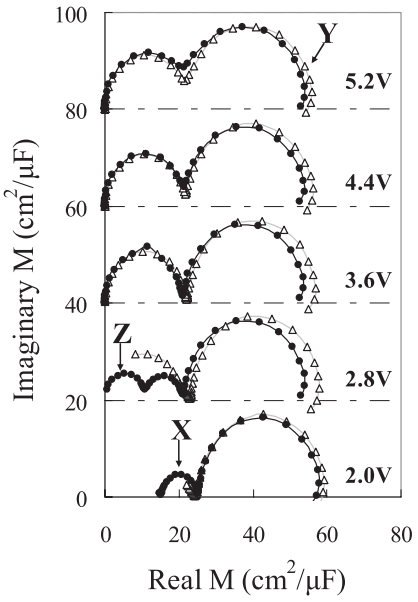

Fig. 7 Cole-Cole plots of Modulus initial (filled-circle) and degraded (open-triangle) PBD-1 doped devices. Each data is shifted upwards by 20 $cm^2/\mu F$ for clarity.

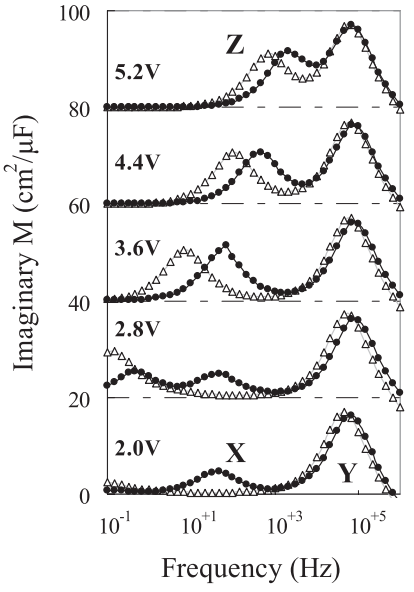

Fig. 8 Bode-plot of imaginary part of Modulus initial (filled-circle) and after operated for 567 hours (open-triangle) in the PBD-1 doped devices. Each data is shifted upwards by 20 $cm^2/\mu F$ for clarity.

circles and the designed layer thickness, it is concluded that the semicircles of EM and ET layers coalesce in a single semicircle by degradation.

In addition, in order to reveal the change of resistance of each layer, we show a Bode-plot of imaginary part of modulus in Fig. 8. The peak frequencies of the Bode-plot show the reciprocal value of the relaxation times. The peak X disappeared by degradation, and the peak Z shifted to the lower frequency side, remarkably. Considering the fact that the effective layer thickness of the initial and degraded device did not change by degradation, the relaxation times of EM and ET changed to nearly the same value by the increase of the resistance of EM.

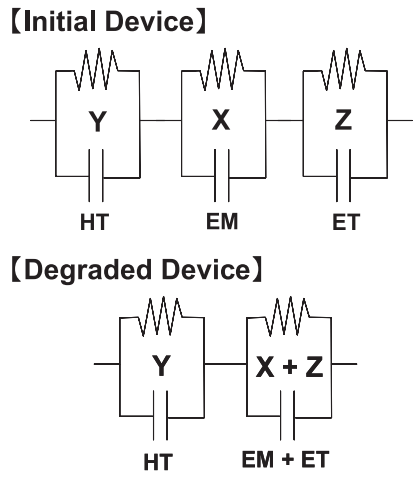

Fig. 9 Equivalent circuit model of initial and degraded devices.

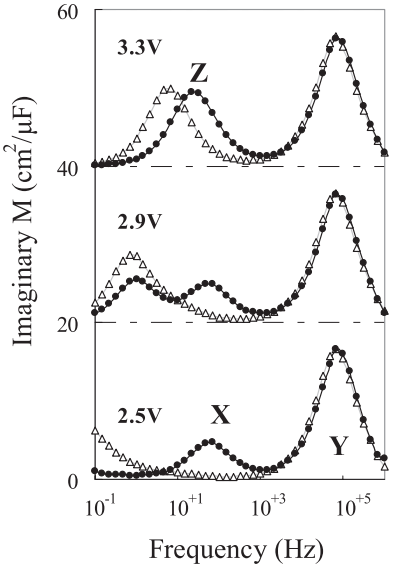

Fig. 10 Bode-plot of imaginary part of Modulus initial (filled-circle) and after operated for 140 hours (open-triangle) in the PBD-1 doped devices. Each data is shifted upwards by 20 $cm^2/\mu F$ for clarity.

Moreover, the shift to lower frequency side was observed also for the peak Y. This fact means that the resistance of HT increased for LT50.

In order to clarify the degradation dynamics more clearly, we also analyzed the device operated for 140 hours (LT85). Figure 10 shows the Bode-plot of imaginary part of the modulus for the devices. The peak X has already disappeared and the peak Z has shifted to the lower frequency side. Nevertheless, the peak Y did not shift. This fact means that the resistance of HT did not increase for LT85.

We summarize IS results as below.

Comparing initial device, the number of semicircles decreased in M-plot of LT50. Because the semicircles of

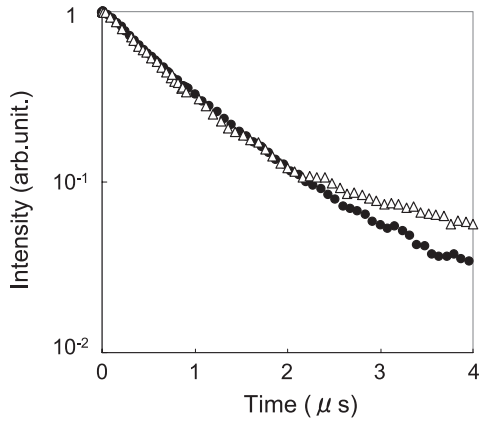

Fig. 11 Transient EL responses of initial (filled-circle) and degraded (open-triangle) devices at 6.4 V.

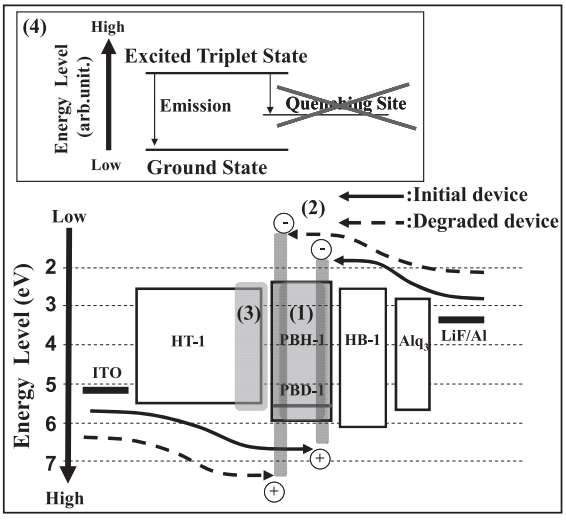

Fig. 12 Scenario of degradation mechanism (1)–(3) of the PBD-1 doped device. No triplet quenching sites are generated, whereas the number of emission sites decreases (4).

EM and ET layers coalesced in a single semicircle due to degradation of the hole conduction in EM. The same phenomena were also observed with LT85. In contrast to the initial device, the peak corresponding to HT shifted to lower frequency side in the Bode-plot of LT50. This means that HT is damaged because the recombination zone shifts to HT side.

3.3 Degradation Analysis by Transient EL

We measured the decay time of the emission by transient EL spectroscopy [16], in order to confirm whether the exciton quenching site was generated as a result of degradation. Figure 11 shows the transient responses of initial and degraded device by transient EL spectroscopy.

Transient EL response of the initial device was coincident with that of the degraded one. The decay times of initial and degraded devices were 0.9 μs, respectively. The result that phosphorescence decay time did not change means that phosphorescence quenching in the device was not so strong and no quenching sites were generated. Nevertheless, reduction of EL was observed with the degraded device. This means that the numbers of the emission sites decreased by degradation.

3.4 Degradation Mechanisms of OLED

From these results, we have made a degradation scenario as follows.
(1) Resistance of EM increases due to degradation of the hole conduction in EM.
(2) The major carriers in EM change from hole to electron and the recombination zone shifts from ET side to HT side.
(3) HT is damaged by the excitons and its resistance increases.
(4) No quenching sites for PBD-1 are generated by degradation in the EM.

4. Conclusion

We applied both IS and transient EL spectroscopy to analyze degradation mechanisms of a phosphorescent blue OLED. From the analysis of the carrier dynamics of OLED by IS, the degradation mechanisms were clarified. From the analysis of transient EL spectroscopy, it is shown that no phosphorescence quenching sites arise in the degraded device but the number of the emission sites themselves decrease by degradation.

From the above results, we have shown that application of both IS and transient EL together provides powerful methods to analyze the degradation process of the OLED.

References

[1] H. Aziz, Z.D. Popovic, N.X. Hu, A.M. Hor, and G. Xu, "Degradation mechanism of small molecule-based organic light-emitting devices," Science, vol.283, pp.1900–1902, 1999.
[2] Z.D. Popovic, H. Aziz, N.X. Hu, A. Ioannidis, and P.N.M.dos Anjos, "Simultaneous electroluminescence and photoluminescence aging studies of tris (8-hydroxyquinoline) aluminum-based organic light-emitting devices," J. Appl. Phys., vol.89, pp.4673–4675, 2001.
[3] D.Y. Kondakov, W.F. Nichols, and W.C. Lenhart, "Structural identification of chemical products and mechanism of operational degradation of OLEDs," SID Tech. Dig., pp.1494–1496, 2007.
[4] D.Y. Kondakov, W.C. Lenhart, and W.F. Nichols, "Operational degradation of organic light-emitting diodes: Mechanism and identification of chemical products," J. Appl. Phys., vol.101, 024512, 2007.
[5] J. Scherbel, P.H. Nguyen, G. Paasch, W. Brütting, and M. Schwoerer, "Temperature dependent broadband impedance spectroscopy on poly-(p-phenylene-vinylene) light-emitting diodes," J. Appl. Phys., vol.83, pp.5045–5055, 1998.
[6] S. Berleb, W. Brütting, and G. Paasch, "Interfacial charges in organic hetero-layer light emitting diodes probed by capacitance-voltage measurements," Synth. Met., vol.122, pp.37–39, 2001.
[7] M. Meier, S. Kang, and W. Riess, "Light-emitting diodes based on poly-p-phenylene-vinylene: impedance spectroscopy," J. Appl. Phys., vol.82, pp.1961–1966, 1997.
[8] M.G. Harrison, J. Grüner, and G.C.W. Spencer, "Investigations of organic eletroluminescent diodes by impedance spectroscopy,

photo-impedance spectroscopy and modulated photovoltage spectroscopy," Synth. Met., vol.76, pp.71–75, 1996.
[9] D.M. Taylor and H.L. Gomes, "Electrical characterization of the rectifying contact between aluminum and electrodeposited poly (3-methylthiophene)," J. Phys. D: Appl. Phys., vol.28, pp.2554–2568, 1995.
[10] M.H. Ho, M.T. Hsieh, K.H. Lin, T.M. Chen, J.F. Chen, and C.H. Chen, "Study of efficient and stable organic light-emitting diodes with 2-methyl-9,10-di (2-naphthyl) anthracene as hole-transport material by admittance spectroscopy," Appl. Phys. Lett., vol.94, 023306, 2009.
[11] C. Hosokawa, H. Tokailin, H. Higashi, and T. Kusumoto, "Transient electroluminescence from hole transporting emitting layer in nanosecond region," Appl. Phys. Lett., vol.63, pp.1322–1324, 1993.
[12] J. Pommerehne, H. Vestweber, Y.H. Tak, and H. Bässler, "Transient electroluminescence from single and double layer light emitting diode (LEDs) based on polymer blends," Synth. Met., vol.76, pp.67–70, 1996.
[13] M. Funahashi, H. Yamamoto, N. Yabunouchi, K. Fukuoka, H. Kuma, C. Hosokawa, E. Kambe, T. Yoshinaga, T. Fukuda, and Y. Kijima, "Highly efficient fluorescent deep blue dopant for "Super Top Emission" device," SID Tech. Dig., pp.709–711, 2008.
[14] S.W. Tsang, S.K. So, and J.B. Xu, "Application of admittance spectroscopy to evaluate carrier mobility in organic charge transport materials," J. Appl. Phys., vol.99, 013706, 2006.
[15] H.C.F. Martens, H.B. Brom, and P.W.M. Blom, "Frequency-dependent electrical response of holes in poly (p-phenylene vinylene)," Phys. Rev. B, vol.60, pp.R8489–R8492, 1999.
[16] M.A. Baldo and S.R. Forrest, "Transient analysis of organic electrophosphorescence: Transient analysis of triplet energy transfer," Phys. Rev. B, vol.62, pp.10958–10966, 2000.

Toshinari Ogiwara received the master degree in Physical Chemistry from Tohoku University, Japan, in 2006. He has studied the magnetic field effect of photocurrent in polymer materials. He joined Idemitsu Kosan Co., Ltd., Japan, in 2006. Since then, he has been engaged in the research and development of phosphorescent OLED materials.

Jun-ichi Takahashi received the M.Sc. degree in plasma physics from Kyoto University in 1985 and Ph.D. degree in laser spectroscopy from Hokkaido University in 2003. During 2001 to 2005, he joined CREST (Hanamura pj.) and ERATO (Koshihara pj.) of JST, respectively. He now joins Idemitsu Kosan Co. Ltd. His present research interests include material science of organic and inorganic materials for electric devices.

Hitoshi Kuma joined Idemitsu Kosan Co., Ltd. in 1990 after graduating from Kyoto University with a master degree in Physical Engineering. After the research of ferroelectric liquid crystal panels for ten years, he has been engaged in the development of OLED materials since 2000. His major is optical and electronic property of organic materials and physical analysis of electro-optical devices.

Yuichiro Kawamura earned his Ph.D. on Material Engineering at Osaka university in 2002. He has studied the application of a heavy metal complex for Organic Light Emitting Diodes (OLEDs) since his master degree. After conducting the photophysical analysis of organic semiconductors in several research groups, he joined Idemitsu Kosan Co., Ltd. in 2007. Now he is engaged in the development of OLEDs.

Toshihiro Iwakuma is currently leading a research and development team to create cutting-edge organic materials for high-performance phosphorescent OLEDs as a senior researcher at Idemitsu Kosan Co., Ltd. Prior to joining Idemitsu Kosan in 1991, He received his B.S. (1986), M.S. (1988) and Ph.D. (1991) degrees in organic chemistry from Graduate School of Science, Tohoku University, Japan. He has over 100 patents, pending patents and publications in the fields of OLED devices/materials and ferroelectric polymer liquid crystals. He is a member of SID.

Chishio Hosokawa joined Idemitsu Kosan Co., Ltd. in 1986 after graduating from Kyoto University with a master degree in physics. Almost immediately he started research on organic light emitting diodes (OLEDs) and thus became one of the pioneer researchers in this field in Japan. He has been engaged in the development of OLED technology ever since. The prospect for practical applications, particularly in full-color displays, has been largely hinged on resolving the blue instability problem. To this end, Hosokawa and his group at Idemitsu Kosan resolved the problem. He is a fellow of Society for information Display (SID).